JOURNAL OF CATALYSIS 105, 499–510 (1987)

CO Hydrogenation on Ru/Al_2O_3: Selectivity under Transient Conditions

X. ZHOU AND ERDOGAN GULARI[1]

Chemical Engineering Department, University of Michigan, Ann Arbor, Michigan 48109

Received October 7, 1986; revised January 26, 1987

Transient response and isotopic tracer techniques were used to investigate the surface coverages of the reactants and the selectivity of ruthenium/alumina catalysts in CO hydrogenation. Two forms of carbon—active carbidic carbon, C_α, and hydrogen-containing alkylic carbon, C_β—are found to be present on the catalyst surface. Approximately 0.1 monolayer of C_α is deposited on the catalyst through the dissociative chemisorption of CO. C_β is formed only in the presence of hydrogen. Unlike C_α, the amount of C_β on the catalyst surface is found to increase continuously. Under varying partial pressures of CO and H_2 the surface coverage of C_α changes much less than the overall rate of reaction. In addition to C_α and C_β, the catalyst surface also contained approximately 0.7 monolayer of CO and 0.1 to 0.2 monolayer of inactive carbon. Measurements of product distributions of C_α and C_β during the hydrogen titration transients show that for C_α the Schultz–Flory distribution is obeyed. In contrast, C_β products do not follow the same distribution. The relative selectivities of the two species of carbon during hydrogen titration transients were very different. C_β titration produced normal and branched alkanes in comparable amounts. No alkene is produced from C_β. C_α titration produced primarily normal alkenes and alkanes. Our results also show that the chain propagation step is much faster than the other steps in hydrocarbon synthesis (Fischer–Tropsch synthesis) and that CO dissociation is not the rate-limiting step.

INTRODUCTION

Surface carbon has been identified as an important intermediate in hydrocarbon synthesis (Fischer–Tropsch synthesis) from CO and H_2 over group VIII metals (*1–11*). Using transient response isotopic tracing and NMR, Bell and co-workers (*3–7*) have identified as many as three forms of surface carbon on unsupported Ru powder and Ru/SiO_2: very active carbidic carbon, C_α, formed by the dissociation of CO in the presence or absence of H_2; less active hydrogenated carbon, C_β, formed from C_α in the presence of H_2; and inactive graphitic carbon. Surface coverage of C_α was found to reach steady state very quickly, whereas C_β coverage increased continuously with time (*3*). Winslow and Bell (*4*) and Duncan *et al.* (*5, 7*) also showed that C_β was alkylic in nature with a hydrogen-to-carbon ratio of 1.8 to 2.4 (*4*) and an average chain length of four to six carbons (*7*). On unsupported Ru powder C_α and C_β were found to produce mainly higher hydrocarbons and methane (*4*).

In terms of its steady-state product distribution Ru/Al_2O_3 is intermediate between unsupported Ru powder (producing mostly higher hydrocarbons) and SiO_2-supported Ru (producing mostly methane). Our goals in this research project were (1) to see if Ru/Al_2O_3 behaved differently than Ru powder and Ru/SiO_2 in terms of the surface coverage and activity of the various forms of surface carbon; (2) to follow the transients in the higher hydrocarbons, as well as methane, to see if there is any difference between the products of different surface carbon species; and (3) to obtain mechanistic information on CO hydrogenation.

[1] To whom correspondence should be addressed.

0021-9517/87 $3.00

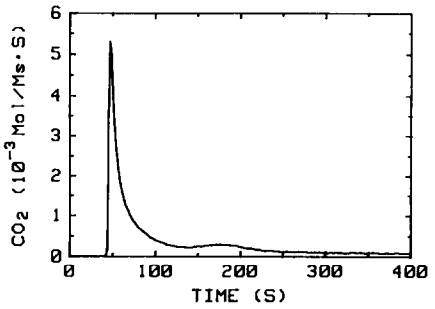

FIG. 1. CO_2 transient from CO disproportionation on a "clean" catalyst. The catalyst was pretreated as follows: H_2 (1500 s, 563 K) → He (1000 s, 563 K) → cool to 451 K in flowing He. The transient was obtained when a step-up of CO was sent into the reactor at 451 K and atmospheric pressure.

EXPERIMENTAL

The experimental setup is composed of a gas flow control system, a Balzers quadrupole mass spectrometer, and an HP 5890A gas chromatograph. The system control and data acquisition were accomplished with an HP 9836 computer.

Two reactors, one containing a monolithically supported catalyst and one glass reactor containing approximately 400 mg of catalyst, were used to obtain all the transient response data. The operation of the reactor system with the monolithically supported catalyst is described in detail elsewhere (*12*). Catalyst preparation and pretreatment procedure involved impregnation with a solution of ruthenium chloride (from Alfa Products) and reduction in flowing hydrogen for 4 h at 473 K. Dispersions of the catalysts used in this study were between 17% (monolithically supported) and 40% (powder).

Before the transient response experiments the catalyst was broken in with a mixture of CO and H_2 for 5 h at steady state. A typical transient response experiment involved the following feed programming: (1) reduction in flowing hydrogen for 2000 s; (2) pretreatment with either pure CO or a mixture of CO and H_2 for the desired amount of time; (3) a short-time purge with helium or argon to clean out the gas phase; (4) feeding in a CO with different isotope of carbon, if an isotope-exchange experiment was being carried out; (5) feeding in a step of hydrogen (or deuterium) and recording the transients.

The gases used were H_2 (99.99%), He (99.995%), Ar (99.9%), all from Air Products, and CO (99.99%) from Matheson Gas Products. Isotopes were D_2 (99.5%) and ^{13}CO (90%), both from MSD Isotopes. All gases were used without further purification.

RESULTS

A. Transient Response Experiments with CO Pretreatment Only

Figure 1 shows a typical CO_2 transient when CO disproportionation occurs on a reduced and helium-purged catalyst surface. The initial rise and decay of the CO_2 signal are very sharp, evidence for a high rate of CO dissociation, even at a fairly low temperature. A smaller second peak is also clearly visible after the first peak has decayed. The amount of carbidic carbon deposited on the catalyst surface, calculated from the area of the CO_2 transient, reached a maximum value of 0.10–0.12 monolayer after 200 s.

The next set of experiments was carried out after pretreating a clean catalyst with pure CO at atmospheric pressure. In this investigation "clean" catalyst means that the catalyst was reduced under pure H_2 and then purged by Ar or He at ~563 K to desorb the chemisorbed hydrogen. Figure 2 shows the typical mass 15 (CH_3^+, primarily due to methane but having some, less than 10%, contribution from the cracking of the higher hydrocarbons) and mass 27 ($C_2H_3^+$, primarily due to ethane and ethylene but having some, less then 20%, contribution also from propane and butane under our experimental conditions) transients obtained by titrating the CO-pretreated catalyst with hydrogen. The mass 27 transient is a single sharp peak, but the mass 15 transient is significantly broader.

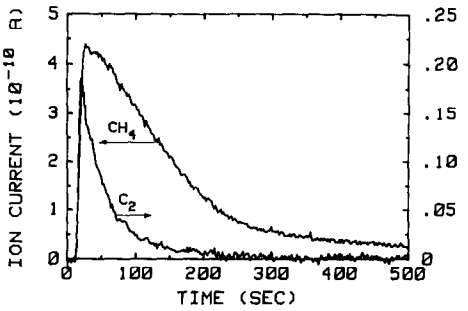

FIG. 2. CH_4 and C_2H_6 transients for H_2 titration of a CO-pretreated catalyst. The transients were obtained by using the mass spectrometer signals for mass fragments 15, CH_3^+, and 27, $C_2H_3^+$. The mass spectrometer signals were calibrated with the methane and ethane GC peaks. Reaction conditions: T = 451 K, atmospheric pressure. Gas delivery program: CO (500 s) → Ar (80 s) → H_2 (500 s).

Through isotope-exchange experiments, Winslow and Bell (*3*) have found that hydrogenation of adsorbed CO makes no contribution to mass 27 and higher mass transients. Taking advantage of this fact we studied the behavior of carbidic carbon, formed by dissociative chemisorption of CO in the absence of H_2, through the higher hydrocarbon transients. By a series of experiments with different CO exposure times, the total area under the mass 27 and higher mass transient peaks was found to level off in 200 s. This means that at this temperature, 451 K, the surface coverage of carbidic carbon reaches its maximum value within 200 s, in agreement with the CO_2 disproportionation results. Integration of only the mass 27 and higher transients yielded a 4–5% surface coverage for carbidic carbon.

To separate the reservoirs of carbon contributing to the methane transient, molecularly adsorbed ^{13}CO was exchanged with ^{12}CO before the introduction of deuterium into the reactor. This process results in the exchange of molecularly adsorbed CO without changing the composition of surface carbon significantly (*3*). The transients of mass 21 ($^{13}CD_4$) formed by hydrogenation of deposited $^{13}C_\alpha$) and mass 20 ($^{12}CD_4$ formed by hydrogenation of chemisorbed ^{12}CO) given in Fig. 3 show the relative activity and quantitative contributions. The shape of the mass 21 transient is very similar to that of the mass 27 transient of Fig. 2 and suggests that there may be two characteristic times governing the decay, a sharp initial decay followed by a much slower decay, but the evidence is not conclusive. The total area of the mass 21 transient is about one-twentieth of the mass 20 transient, or 0.04–0.05 monolayer. Summing the mass 21 and higher mass transients gives a carbidic carbon surface coverage of ~0.10 monolayer, in good agreement with the CO disproportionation result. Figure 3 together with Fig. 2 shows that the contribution of surface carbon to the mass 15 transient is small compared with the contribution coming from the hydrogenation of molecularly adsorbed CO and that the transients of mass 15 and higher arising from hydrogen titration of carbidic carbon all have the same shape and time dependence.

By monitoring the transients of mass fragments 31, 33, and 35 (resulting from fragmentation of $^{12}C^{13}CD_6$), we found out that even though the surface already had an equilibrium coverage of ^{13}C under the conditions of our experiment [lower temperature than those of Winslow and Bell (*3*)] some ^{12}C did form on the surface.

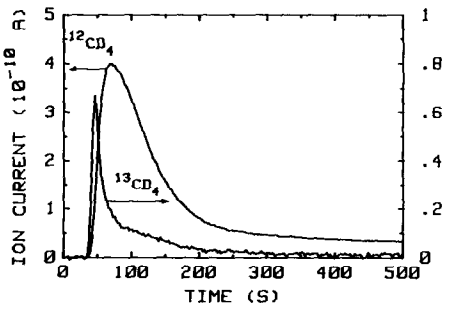

FIG. 3. $^{12}CD_4$ (mass 20) and $^{13}CD_4$ (mass 21) formation transients for D_2 titration after isotope exchange of the molecularly adsorbed ^{13}CO by ^{12}CO. Reaction conditions: T = 433 K, P = 550 Torr. Gas delivery sequence: ^{13}CO (600 s) → He (200 s) → ^{12}CO (300 s) → He (200 s) → D_2 (500 s).

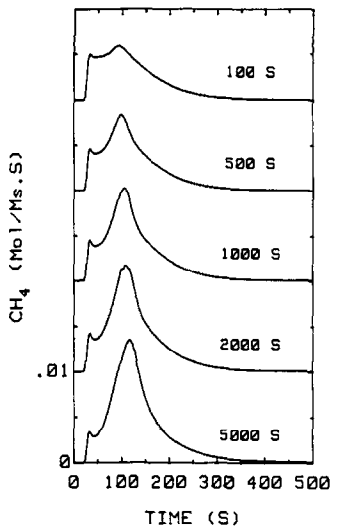

FIG. 4. CH_4 transients obtained after hydrogen titration of the catalyst exposed to a reactive mixture of CO + H_2 for different times. Reaction conditions: T = 451 K, atmospheric pressure. Gas delivery sequence: CO + H_2 (CO/H_2 = $\frac{1}{3}$) varied times → He (80 s) → H_2 (500 s).

We also observed that if the residual hydrogen left on the catalyst, from the reduction cycle, was not completely removed by Ar or He purging the initial slopes of all the transients due to hydrocarbons were much steeper.

B. Transient Response Experiments with CO/H_2 Pretreatment

Figure 4 shows the methane transient as a function of pretreatment time after pretreating with CO + H_2. If we compare Fig. 4 to Figs. 2 and 3 we see a distinct difference. As the pretreatment time increases we have a sharp second peak not present in Figs. 2 and 3. Following the notation of Bell and co-workers the first peak is labeled the C_α peak and the second peak is labeled the C_β peak. The C_α peak is believed to be due to the hydrogenation of carbidic carbon formed by the dissociation of CO. The C_β peak is assigned to the products resulting from hydrogenation of already-hydrogen-containing surface carbon formed only in the presence of CO and hydrogen together. C_β is apparently less active than the carbidic carbon, C_α (*1, 3*). The second, C_β, peak of Fig. 4 is much larger than the first one and keeps increasing in size even after 5000 s of pretreatment time.

Figure 5 shows the C_2^+ (ethane and higher hydrocarbons) transient as a function of pretreatment time. Again we have two distinct peaks. The small C_α peak appears at the same time as in Fig. 2 and the second peak, due to C_β, increases in size with pretreatment time. The C_β peak position shifts to longer times with increasing pretreatment time. Unlike the mass 15 transients shown in Fig. 4 the C_α and C_β peaks of mass 27 transients are clearly separated.

To quantitate the relative amounts contributed by the C_α and C_β peaks we integrated the areas under each peak as a function of pretreatment time. The results are shown in Fig. 6. The amount of C_β carbon on the catalyst surface increases with pretreatment time. The amount of C_α carbon, on the other hand, reaches its maximum

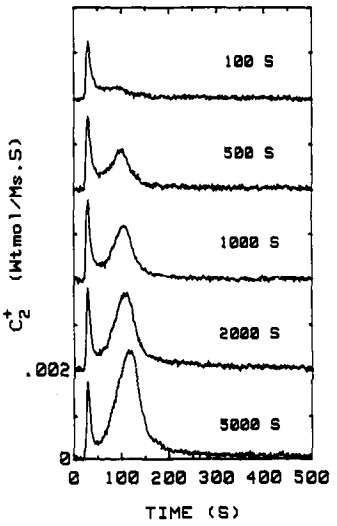

FIG. 5. C_2^+ (ethane and higher-molecular-weight hydrocarbons) transients obtained after hydrogen titration of the catalyst exposed to a reactive mixture of CO + H_2 for different pretreatment times. Reaction conditions: T = 451 K, atmospheric pressure. Gas delivery sequence: CO + H_2 (CO/H_2 = $\frac{1}{3}$) varied times → He (80 s) → H_2 (500 s).

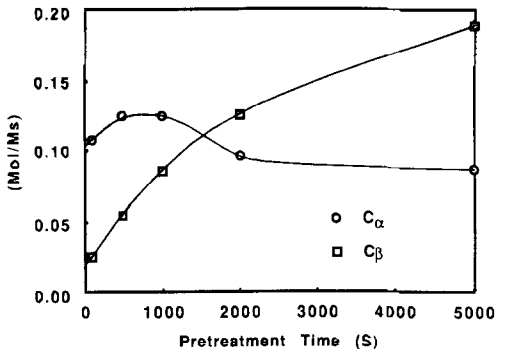

FIG. 6. Surface coverage as a function of reaction time. The amount of C_α was obtained by integrating the C_α peaks of Figs. 4 and 5. The amount of C_β was obtained by integrating the second peaks of Fig. 5 only. Reaction conditions: T = 451 K, atmospheric pressure. Gas delivery sequence: CO + H_2 (CO/H_2 = $\frac{1}{3}$) varied times → He (80 s) → H_2 (500 s).

value very rapidly and then decreases slowly. This decrease in C_α could be due to occupation of some of the surface sites by C_β or to inactive graphitic carbon formation.

We also tried to separate the contributions of molecularly adsorbed CO to the mass 15 peak from that of the C_β. However, only in the 383 K transient was the mass 15 peak due to adsorbed CO barely distinguishable from the mass 15 peak due to C_β carbon (CH_3^+ formed from adsorbed CO came out earlier).

Figure 7 shows the effect of inert gas purging on the C_2^+ transient. As the purge time increases, the C_β peak moves to shorter times and overlaps with the C_α peak. Within error we did not detect any increase in the area of the C_α peak, but this conclusion is based on the difficult separation of overlapping peaks and is for the temperature we were using, 433 K. Integration of the CH_4 and C_2 transients showed that the total amount of higher hydrocarbons did not change, but the amount of methane decreased by approximately 25% upon prolonged purging. This is to be expected since adsorbed CO, which is slowly desorbed during the purge, contributes significantly to the methane transient but not to the higher hydrocarbon transient. The observed decrease corresponds to a loss of approximately 0.5 monolayer of CO.

C. ^{12}CO–^{13}CO Isotope Exchange Transients

To determine the nature of growth and breakdown of C_β carbon on the catalyst surface we carried out an isotope-exchange transient with the feed program $^{12}CO + D_2$ (3000 s) → He (50 s) → vacuum (50 s) → ^{13}CO (600 s) → He (100 s) → D_2 (400 s). In comparing the transients for masses 32 and 33, corresponding to $^{12}C_2D_4^+$ and $^{12}C^{13}CD_4^+$ fragments, we observed that mass 33 had no contribution from the C_β peak, whereas the mass 32 transient had contributions from both C_α and C_β peaks. In general, all the odd-number mass fragments, which represent the molecules with both ^{12}C and ^{13}C in the skeleton, exhibited only the C_α peak. Clearly, when there is no gas-phase hydrogen, no carbon exchange takes place between the C_α and C_β reservoirs.

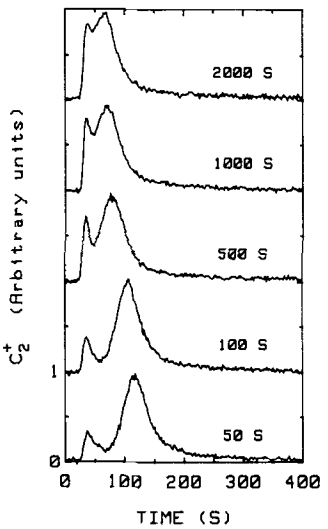

FIG. 7. Inert gas purging effect on C_2^+, mass 27, due to ethane and higher-molecular-weight hydrocarbons, transient. Reaction conditions: T = 433 K, atmospheric pressure. Gas delivery sequence: CO + H_2 (CO/H_2 = $\frac{1}{3}$, 1500 s) → He (t varying) → H_2 (500 s).

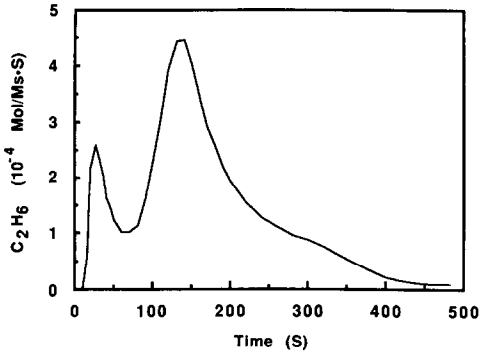

FIG. 8. Ethane transient obtained by repetitive sampling with the GC. Reaction conditions: T = 433 K, atmospheric pressure. Gas delivery sequence: CO + H_2 (⅓, 2500 s) → He (80 s) → H_2 (500 s).

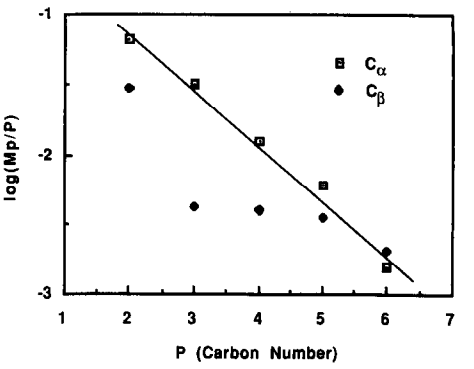

FIG. 9. Schultz–Flory plots for the products of C_α and C_β as determined by GC analysis of samples taken at the respective peak positions. Reaction conditions: T = 433 K, atmospheric pressure. Gas delivery sequence: CO + H_2 (⅓, 2500 s) → He (80 s) → H_2 (500 s).

D. Selectivity during Hydrogen Titration Transients

While the mass spectrometer transients are informative with respect to the time dependence, it is difficult if not impossible to obtain quantitative individual transients for the C_2 and higher hydrocarbons from the mass spectrum results. To investigate the selectivity question, hydrogen titration transients were obtained with a GC. Very reproducible repetitive GC sampling was accomplished by triggering the GC by the computer, which was also monitoring the mass spectrometer signal. Figure 8 shows the ethane transient after CO + H_2 pretreatment. The overall shape of Fig. 8 is very similar to that of Fig. 5; however, the higher quality of the data shows a distinct shoulder in the rate of ethane production around 300 s. A similar shoulder was observed for the higher hydrocarbons.

Selectivity measurements with the GC also provided us with a means of determining the product distribution at any time during the hydrogen titration transient. Figure 9 shows the Schultz–Flory (SF) plots for the C_α and C_β peaks. Due to the large contribution of the chemisorbed CO to methane, it is not included in the curve fitting; thus the intercept may not be meaningful. C_α products fit the Schultz–Flory distribution quite well. In contrast, C_β products do not appear to follow the Schultz–Flory distribution.

Figure 10 shows the *n*-butane and isobutane transients. It is of interest that the relative ratios for the C_α and C_β peaks are quite different. The relative amount of branched product from C_β is much higher than that from C_α. Similar behavior was seen for the C_5 and higher hydrocarbon products. Olefins were detectable only in the C_α peak.

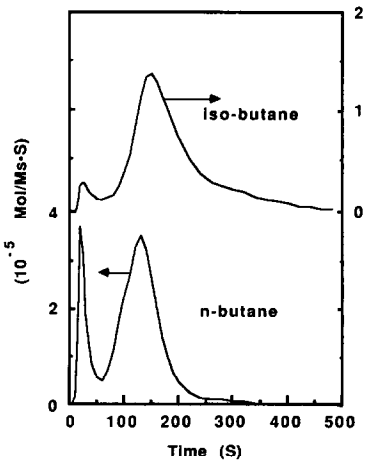

FIG. 10. Linear and branched butane transients obtained by GC. Reaction conditions: T = 433 K, atmospheric pressure. Gas delivery sequence: CO + H_2 (⅓, 2500 s) → He (80 s) → H_2 (500 s).

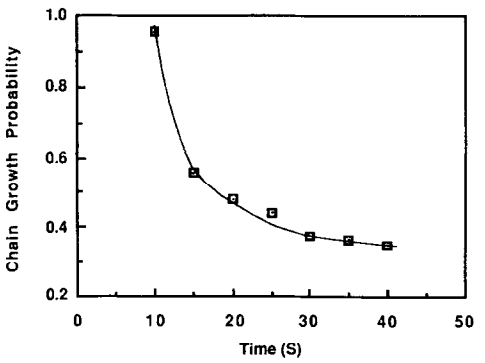

FIG. 11. The change in the chain propagation probability of C_α during a hydrogen titration transient of CO + H_2-pretreated catalyst surface. Reaction conditions: T = 433 K, atmospheric pressure. Gas delivery sequence: CO + H_2 ($\frac{1}{3}$, 2500 s) → He (80 s) → H_2 (500 s).

One important piece of information we obtained from the GC transients was the rate of the chain propagation step versus the other steps. By making S–F plots at several time points along the C_α transient we observed that the product distribution obeyed the S–F distribution quite well for all the points (correlation coefficients of 0.98 or better). Figure 11 shows the variation of the chain growth probability as a function of time. At the beginning of the transient the probability of chain growth is almost one but decreases very quickly to a low value of 0.36. At the peak of the transient the chain growth probability was approximately 0.45–0.5. The C_α products, obtained after pretreating the catalyst surface with CO only, also obeyed the S–F distribution and the chain growth probabilities were comparable to the probabilities for C_α deposited in the presence of H_2.

Since the surface coverage of C_β increases continuously with time, it is of interest to determine if the increase in C_β is due to an increase in surface coverage or to an increase in the average chain length. Assuming that the carbon number distribution of the titration products is related to the chain length of the C_β on the catalyst surface, measuring the product distribution of C_β as a function of pretreatment time with CO and H_2 should tell us if the average chain length increases with time or not. The results scanning the pretreatment time range of 100 to 5000 s showed a moderate increase (C_4/C_2 ratio increasing by more than 30%) toward higher carbon numbers. Unfortunately, the chain growth probability for the C_α products also increases slightly during the same time period, making any conclusions about the changing C_β product distribution qualitative at best. A second reason for only a moderate increase may be the hydrogenolysis of the long chains.

E. H_2–D_2 Isotope Exchange Results

Figure 12 shows typical H_2, DH, CDH_3, and mass 30 (from C_2H_6, C_2DH_4, $C_2D_2H_2$, C_2D_3 fragments) transients after D_2 titration of a CO + H_2-pretreated catalyst. Two peaks are present in each transient. In analogy with hydrocarbons, the first and the second peaks of H_2 and DH were labeled as H_α and H_β by Winslow and Bell (*13*). H_α is

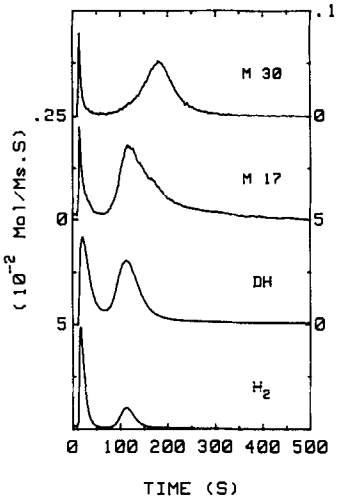

FIG. 12. D_2 titration transients of a CO + H_2-pretreated catalyst. The C_α peak heights were converted into absolute concentrations by calibrating with the GC transients (mass 17 by methane and mass 30 by the sum of C_2^+ peak areas of the GC transients). Reaction conditions: temperature, 443 K. Gas delivery sequence: H_2 + CO (p_{H_2} = 380 Torr, p_{CO} = 127 Torr, p_{Ar} = 253 Torr, 2.5 h) → Ar (100 s) → D_2 (600 s).

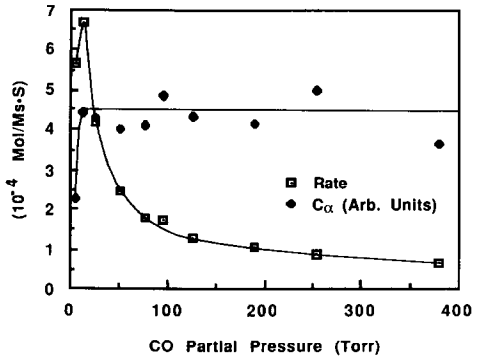

FIG. 13. Carbidic carbon, C_α, and the total steady-state reaction rate as functions of CO partial pressure. Raction conditions: temperature, 443 K. Gas delivery sequence: H_2 + CO + Ar (2.5 h) → Ar (100 s) → D_2 (600 s). H_2 partial pressure was kept constant at 380 Torr while the CO partial pressure changed from 0 to 380 Torr. Argon was used to make up the total pressure to 760 Torr. The total amount of carbidic carbon was determined by integration of all the C_α transients.

due to chemisorbed hydrogen on the catalyst surface and H_β is due to exchanging of some of the hydrogen associated with C_β. In contrast to the results of Winslow and Bell (*4*), who only detected completely exchanged CD_4, we were able to detect all the masses from 13 to 50 corresponding to almost every possible combination of H and D in the hydrocarbons originating from both C_α and C_β reservoirs.

To our knowledge there has not been any direct experimental studies that reveal how surface hydrogen coverage changes as a function of gas-phase composition and how this change affects the reaction rate. In an attempt to answer these questions we studied the changes in hydrogen surface coverage, with varying gas-phase composition, but the results were difficult to interpret due to interference from the surface hydroxyls of the support. A series of experiments similar to that in Fig. 12 was carried out. The total reaction rate measured as a function of CO partial pressure is plotted in Fig. 13. To measure the C_α coverage change, the α peaks of mass numbers 17 (C_1 segment from CH_3D^+ and CHD_2^+) and 30 (from C_2H_6, C_2DH_4, $C_2D_2H_2$, C_2D_3 fragments) were integrated and calibrated with the GC measurements of methane and C_2^+ concentrations. We found that mass 17 had almost no contribution from the hydrogenation of surface CO, which produced mainly CD_4 during the D_2 titration. The area under the mass 17 transient decreased, and the area under the mass 30 transient increased, with increasing CO partial pressure. The total C_α, estimated by adding one C_1 area and two C_2 areas, remained approximately constant over a wide range of CO partial pressures, as shown in Fig. 13. At very low CO partial pressures, a negative correlation between the rate of reaction and C_α coverage is observed.

In an effort to determine whether graphitic, inactive carbon was being formed on the catalyst surface, we ran the reaction at 473 K for a day and then hydrogen titrated the catalyst. Under isothermal conditions we could not detect any hydrocarbon peaks after the C_β peak; however, after allowing hydrogen to flow through the reactor at 473 K for 24 h, and then increasing the temperature a methane peak was detected in the effluent between 523 and 553 K. The total amount of methane corresponded to 10% of a monolayer carbon coverage.

DISCUSSION

A. Carbidic Carbon, C_α

The CO_2 transient in Fig. 1 shows that CO dissociation on a clean catalyst surface is a very fast process and CO dissociation almost ceases after 200 s when ~12% of the surface is covered by deposited carbon. In agreement with the findings of Winslow and Bell (*3*) our hydrogen titration experiments given in Fig. 2 also show that the carbidic carbon is very active in hydrogenation. Integration of the hydrocarbon transients also yield a surface coverage of approximately 10 to 12% of a monolayer, proving that in the temperature range 413–453 K most of the deposited carbon is in carbidic form, though at higher temperatures some graphite may form on the surface (*14*). Since CO

dissociation by the Boudouard reaction is almost completely irreversible (*8*) the limitation must be due to the number of sites available on the surface. In their experiments with single crystal surfaces, Tamaru *et al.* (*15*) found that carbidic carbon equivalent to ~4% of the surface atoms was formed on a Ru(1,1,10) stepped plane, whereas no carbidic carbon was formed on a Ru(001) flat plane. Based on these results, they proposed that CO dissociation occurs only at the low coordination sites. If dissociative chemisorption is site limited, it should be possible to measure a change in the C_α coverage with crystallite size.

C_α hydrogenation products obey the Schultz–Flory distribution during the transients (Fig. 9). This can happen only if the chain propagation step is in quasi-steady state or much faster than the rate-determining step: either initiation or termination. If the termination step is slower than the carbon decomposition, or initiation, step, some of the carbon monoxide isotope used to exchange the molecularly adsorbed CO should dissociate (as sites become available) and participate in the chain propagation step, resulting in mixed carbon isotope products. This hypothesis is nicely verified by the detection of the odd-numbered mass fragments 31, 33, and 35, all due to C_2 or higher carbon species containing both ^{12}C and ^{13}C, in the C_α peak.

When we pretreat the surface with both CO and H_2 (Figs. 4 and 5) the coverage of C_α is again ~12%. If we compare the shapes of the C_α peaks in Fig. 2 with that in Fig. 5 carefully, we find that the C_α peak of Fig. 5 is sharper, even though the amount of C_α deposited on the catalyst is roughly the same, in the presence or the absence of hydrogen. One possible explanation of this difference is that carbon deposition on a clean surface proceeds by island formation (*16*); therefore the carbidic carbon atoms are closely packed (but not close enough to form graphite). When H_2 is present on the surface, carbidic carbon may deposit in a segregated pattern with hydrogen atoms filling in between, resulting in a higher initial rate of reaction. The third obvious explanation of course is that some of the hydrogen is already on the catalyst surface, and thus there is no lag time due to hydrogen adsorption from the gas phase. With the available evidence it is not possible to choose between the three possibilities.

Our H_2 titration transients provide very useful information on the reaction kinetics. The dependences of the steady-state reaction rate and the C_α coverage of the catalyst on gas-phase composition shown in Fig. 13 demonstrate that the reaction rate has a very strong dependence on the gas-phase composition. As CO partial pressure increases from 12.5 to 380 Torr, the surface coverage of carbidic carbon, C_α, stays almost constant, whereas the total reaction rate decreases from 6.7×10^{-4} to 0.8×10^{-4} mol/Ms·S (moles of surface sites). Obviously, in this range of CO partial pressures the reaction rate is not controlled by CO dissociation. Below 12.5 Torr of CO, both the rate of reaction and the amount of surface C_α increase with CO partial pressure. Thus, the overall reaction rate changes from being CO, or surface C_α, limited to surface hydrogen limited.

We find that the C_α products obey the Schultz–Flory distribution with a changing chain growth probability all along the hydrogen titration transient. The fact that the chain growth probability starts at close to one and decreases smoothly as the surface C_α is consumed, as shown in Fig. 11, implies that the propagation step is very fast compared to the termination step. A corollary is that the distribution is established during the hydrogenation reaction and not during the carbon deposition. Otherwise, the products would not obey the Schultz–Flory distribution and we would have reproducibility problems in measuring the product distributions during the transients. Obeying the Schultz–Flory distribution even when there is very little C_α on the surface implies very high surface mobilities for the intermediates or localized regions of C_α

on the catalyst surface. Based on the data it is not possible to choose between the two.

Figure 11 provides further insight into understanding the selectivity question in Fischer–Tropsch synthesis. It shows that the chain propagation probability on Ru is determined solely by the availability of C_α versus surface hydrogen. One can increase the average molecular weight of the products either by increasing the surface coverage of C_α or by decreasing the hydrogen availability. The surface coverage of C_α can be increased by either increasing the rate of production of C_α, increasing the CO dissociation rate, or by slowing down the consumption of C_α, decreasing the surface concentration of hydrogen. The last option, however, results in a lower overall rate of reaction by slowing down the termination step. Since many promoters, such as alkali metals, are found to slow down the overall rate of reaction significantly they must be increasing the average molecular weight by decreasing the surface hydrogen concentration.

On almost all common Fischer–Tropsch synthesis catalysts the product distribution is found to obey the Schultz–Flory distribution. Our observation that only the C_α hydrogenation products follow Schultz–Flory distribution implies that at steady state the majority of the hydrocarbons are formed by C_α.

B. Alkylic Surface Carbon C_β

Agreeing with the previous studies (*3, 4, 17*) our results also show that when the catalyst is pretreated with CO and H_2 together, a new and apparently less active form of hydrogenated surface carbon, C_β, is formed. The accumulation of C_β is probably due to a part of C_α reacting with hydrogen and staying on the surface. From Fig. 8 it can be seen that under steady-state reaction conditions the initial rate of C_β formation increases with the CO partial pressure. Thus, the existence of adsorbed CO is essential to the formation of C_β.

Using a ruthenium carbonyl solution, Pichler *et al.* (*18*) observed that the rate of growth of polymethylene chains attached to ruthenium increased dramatically with CO pressure. Under Pichler's reaction conditions, "living polymers" (i.e., polymers that can continue to grow any time as long as the monomer, CH_2, is available) were present. Based on IR evidence, the growth site was deduced to be an alkylruthenium carbonyl $[CH_3(CH_2)_nCH_2\text{–}Ru(CO)_x]$, where x varies from 3 to 5 and n is a large number. Our own *in situ* IR results (to be published separately) indicate that the $-CH_2-$ to $-CH_3$ ratio of C_β increases with time and CO partial pressure. Parenthetically, we note that Pichler's observations were unique to ruthenium and could not be repeated with other catalysts. One explanation for the necessity of CO chemisorbed on the same ruthenium atom may be electronic: the carbonyl ligands reduce the electron density at the ruthenium atom and, as a result, strengthen the carbon-to-ruthenium bond. This model would also explain (1) why C_β hydrogenation does not start until a certain amount of the chemisorbed CO is hydrogenated and (2) why the reactivity of C_β increases after prolonged purging (and thus desorbing some of the adsorbed CO) with an inert gas. We must, however, point out that most of the evidence is indirect and it is possible to have many other models yielding similar results.

According to our isotope-exchange transients, in the absence of hydrogen, changing the gas-phase CO changes the isotopic composition of C_α but not of C_β as evidenced by the lack of C_β peaks for the odd-numbered mass fragments containing both ^{12}C and ^{13}C. This observation can be explained if, when there is significant surface coverage of CO, insertion into a C_β chain occurs only via a methylene group (*3, 4*). Observation of mixed isotope containing species is also unlikely if, instead of going through the chain propagation step, C_β desorption proceeds through a hydrogenolysis step during which chain breakage rather than growth occurs.

The inert gas purging experiment (Fig. 7) shows that at 433 K there is no dynamic equilibrium between C_α and C_β. Unlike the previous report by Winslow and Bell (*4*), we did not see C_β converting back to C_α. What we observed was an increase in the activity of C_β. These results do not necessarily contradict Winslow and Bell's finding (*3*); at the higher temperatures, part of C_β could be dehydrogenated and converted back into carbidic carbon. Alternately, since the hydrogen-to-carbon ratio of C_β is found to decrease (*4*) with increasing temperature, hydrogenolysis of C_β could lead to the formation of olefinic fragments which participate in the chain growth.

If C_β is converted back to C_α, before leaving the catalyst surface, then the product distribution patterns of α and β peaks should be the same. If we assume that C_β consists of C_α hydrogenation products strongly attached to the surface but in dynamic equilibrium with C_α, a simple desorption by hydrogenation should lead to product distributions similar to the C_α product distribution. On the contrary, dramatic differences exist between the two distributions. Unlike the α peak, the β peak contains no detectable olefin and has a high branched-to-linear product ratio. Most importantly, the product distribution of C_β does not follow the Schultz–Flory distribution. We have modified the reaction mechanism proposed by Winslow and Bell (*4*) slightly to account for these possibilities:

$$\mathrm{CO} \rightarrow \mathrm{C}_\alpha \underset{-\mathrm{H}}{\overset{+\mathrm{H},\ \text{Propagation}}{\rightleftharpoons}} \mathrm{C}_x\mathrm{H}_y \xrightarrow{+\mathrm{H},\ \text{Termination}} \text{Product}$$

$$\mathrm{C}_\alpha \overset{+\mathrm{H}}{\rightleftharpoons} \mathrm{C}_\beta \xrightarrow{\text{Hydrogenolysis}} \text{Product}$$

This model can explain the experimental results quite well. If at low temperatures C_β is nothing but terminally bound alkyl hydrocarbon (*18, 19*), significant amounts of olefins should not be expected. Olefins are only produced during hydrogenation of C_α as primary products. The residence time of C_β on the surface is also much longer than that of the C_α products and there is a higher chance of branching (*20*) through rearrangement reactions. During the hydrogenolysis reaction the branched structure will be retained because the tertiary carbon atom is relatively stable on Ru (*21*) resulting in the higher ratio of branched-to-linear products.

We found that during the inert gas purging, desorption of surface CO resulted in a considerable increase in the activity of C_β. It is obvious that surface CO inhibits the hydrogenolysis of C_β. A second explanation (in addition to the one given above for CO stabilization of ruthenium alkyls) is that two sites are needed to rupture a C–C bond in a hydrocarbon chain, a necessary step in desorption, and removal of surface CO opens up new sites for the reaction to take place.

CONCLUSIONS

The mechanism of the Fischer–Tropsch reaction on Ru/Al_2O_3 is very complicated. The reaction starts with CO dissociation on the metal which, probably, can occur only on low coordination sites. These sites make up about 10–12% of the total surface sites of our catalyst. According to our results CO dissociation proceeds at a much faster rate than the termination step on the catalyst surface. Under steady-state reaction conditions and a wide range of CO partial pressures the C_α coverage appears to be constant within experimental error.

The chain propagation step is also found to be very fast compared with the termination step and the products of C_α hydrogenation follow Schultz–Flory distribution even under transient conditions. Therefore the reaction rate on an Ru catalyst under steady-state conditions is limited by the termination step.

In addition to carbidic carbon, alkylic carbon, C_β, is deposited on the surface. In the presence of CO, C_β appears to be much less reactive than C_α toward hydrogenation. It accumulates under reaction conditions and can reach more than a monolayer of equivalent surface coverage. The reac-

tion path of C_β to the products is strongly inhibited by the molecularly adsorbed CO. The products of C_β do not follow the Schultz–Flory distribution and we speculate that hydrogenolysis may be the primary means of desorbing C_β.

ACKNOWLEDGMENTS

We thank one anonymous reviewer for many valuable comments. One of us, E.G., thanks the Chemical Engineering Department of the University of California, Berkeley, for a visiting professor appointment during the time this paper was written and acknowledges the stimulating discussions on FT synthesis with Professor A. T. Bell and his research group. We are grateful to the University Coal Research Program of DOE (Contract DOE-DE-FG22-84PC 71785) and the Catalysis Kinetics Program of NSF (Grant NSF-G-CBT-8513127) for financial support.

REFERENCES

1. Ponec, V., *Catal. Rev. Sci. Eng.* **18**(1), 151 (1978).
2. Bell, A. T., *Catal. Rev. Sci. Eng.* **23**(1), 203 (1981).
3. Winslow, P., and Bell, A. T., *J. Catal.* **86,** 158 (1984).
4. Winslow, P., and Bell, A. T., *J. Catal.* **94,** 142 (1985).
5. Duncan, T. M., Winslow, P., and Bell, A. T., *J. Catal.* **93,** 1 (1985).
6. Duncan, T. M., Winslow, P., and Bell, A. T., *Chem. Phys. Lett.* **102,** 163 (1983).
7. Duncan, T. M., Reimer, J. A., Winslow, P., and Bell, A. T., *J. Catal.* **95,** 305 (1985).
8. Biloen, P., Helle, J. N., and Sachtler, W. M. H., *J. Catal.* **58,** 95 (1979).
9. Underwood, R. B., and Bennett, C. O., *J. Catal.* **84,** 358 (1983).
10. Bianchi, D., Borcar, S., Teule-Gay, F., and Bennett, C. O., *J. Catal.* **82,** 442 (1983).
11. Bianchi, D., Tau, L. M., Borcar, S., and Bennett, C. O., *J. Catal.* **82,** 442 (1983).
12. Barshad, Y., and Gulari, E., *J. Catal.* **94,** 468 (1985).
13. Winslow, P., and Bell, A. T., *J. Catal.* **91,** 142 (1985).
14. Goodman, D. W., and White, J. M., *Surf. Sci.* **90,** 201 (1979).
15. Shincho, E., Egawa, C., Naito, S., and Tamaru, K., *Surf. Sci.* **149,** 1 (1985).
16. Shincho, E., Egawa, C., Naito, S., and Tamaru, K., *Surf. Sci.* **155,** 153 (1985).
17. McCarty, J. G., and Wise, H., *J. Catal.* **57,** 406 (1979).
18. Pichler, H., Firnhaber, B., Kiossis, D., and Dawalla, A., *Makromol. Chem.* **70,** 12 (1964).
19. Yanasaki, H., Kobori, Y., Naito, S., Onishi, T., and Tamaru, K., *J. Chem. Soc. Faradey Trans. I* **77,** 2913 (1981).
20. Henrici-Olive, G., and Olive, S., "The Chemistry of the Catalyzed Hydrogenation of Carbon Monoxide." Springer-Verlag, Berlin/New York, 1984.
21. Machiels, C. J., and Anderson, R. B., *J. Catal.* **58,** 260 (1979).